

Jet Pulse Electrodeposited Ni-SiC Thin Coatings by Using Experimental System Designed for Potential Industrial Application

Wenqing Liu¹, Kedi Jiang^{1,*}, Qiang Li^{1,2}, Chunyang Ma¹, Fafeng Xia¹

¹ College of Mechanical Science and Engineering, Northeast Petroleum University, Daqing 163318, PR China;

² School of Chemistry Engineering, Hanshan Normal University, Chaozhou 521041, China

*E-mail: chunyangandma@163.com

Received: 3 December 2020 / Accepted: 21 January 2021 / Published: 28 February 2021

Ni-SiC thin coatings were prepared by using the jet pulse electrodeposition (JPED) method while the jet rate was determined with the Fluent software. Moreover, the effects of jet rate on the surface topography, microstructure, surface hardness, and wear property of the Ni-SiC thin coatings were examined through scanning electron microscopy (SEM), scanning probe microscopy (SPM), transmission electron microscopy (TEM), X-ray diffraction (XRD), Vickers hardness instrument, and abrasion testing machine. The SiC particles revealed diffraction peaks at 34.1°, 41.4°, and 59.6°, corresponding to the planes of (1 1 1), (2 0 0) and (2 2 0), respectively. The SiC and Ni peaks were observed at 19.5 nm and 50.2 nm, respectively, in the prepared Ni-SiC thin coatings at 3 m/s jet rate. Furthermore, it also exhibited significantly larger microhardness value i.e. 886.65 HV as compared to the Ni-SiC coating obtained at 1 m/s i.e. 730.15 HV. There were certain scratches and slight small-sized pits in the coating surface prepared at 3 m/s. In addition, the Ni-SiC thin coating deposited at 3 m/s processed the highest impedance, indicating the best corrosion resistance among all coatings.

Keywords: Ni-SiC thin coating; jet rate; surface topography; abrasion testing; surface hardness

1. INTRODUCTION

Nowadays, many kinds of metal based composite (MBC) coatings are widely examined because of the outstanding surface properties, including larger surface hardness, excellent corrosion and wear resistance compared to the pure metal coatings [1-6]. And they were proverbially applied in mechanical, chemical, petroleum and protection fields. Generally, MBC coatings could be synthesized via laser cladding, electrodeposition, chemical deposition, jet pulse electrodeposition (JPED) and sputtering

deposition [7-11]. Among these techniques, the JPED is a convenient, simple and inexpensive method for producing MBC coatings. Recently, some reports concerning about JPED-depositing these coatings have been discussed by lots of scholars (domestically as well as abroad). Xia *et al.* [12] expatiated the prefabrication of the Ni-TiN coatings via JPED technique. They found an approximate nanohardness of ~34.5 GPa for the Ni-TiN coatings deposited at 5 g/L. Ma *et al.* [13] successfully prepared Ni-AlN coatings by adopting JPED method. The obtained results showed average surface hardness of 767.9 HV for the Ni-AlN coating. Tian *et al.* [14] reported the preparation of nickel coatings on the carbon steel substrates via JPED method. The results illustrated a smallest grain size of approximately 13.7 nm in the nickel coatings that was deposited at a current density of 39.8 A/dm². Cui *et al.* [15] prepared Ni-SiC composites on Al2519 substrates by using JPED method. According to this report, we improved the experimental device and tried to produce Ni-SiC thin coatings on mild steel substrates.

Although many studies were reported JPED-deposited MBC coatings by scholars at home and abroad, these reports were primarily concentrated on the effects of plating parameters on the microstructure, wear resistance and microhardness of the coating. By comparison, few researches concerning the action mechanisms of different jet rates on JPED-deposited Ni-SiC thin coatings appeared in recent reports. In this work, the Ni-SiC thin coatings were synthesized using JPED technique with different jet rates. The basic message of plating solution field was achieved by using numerical simulation. Besides, the microstructure, surface topography, microhardness and wear resistance of Ni-SiC thin coatings were also discussed by using scanning electron microscopy (SEM), transmission electron microscopy (TEM), scanning probe microscopy (SPM), X-ray diffraction (XRD), Vickers hardness instrument, and abrasion testing machine.

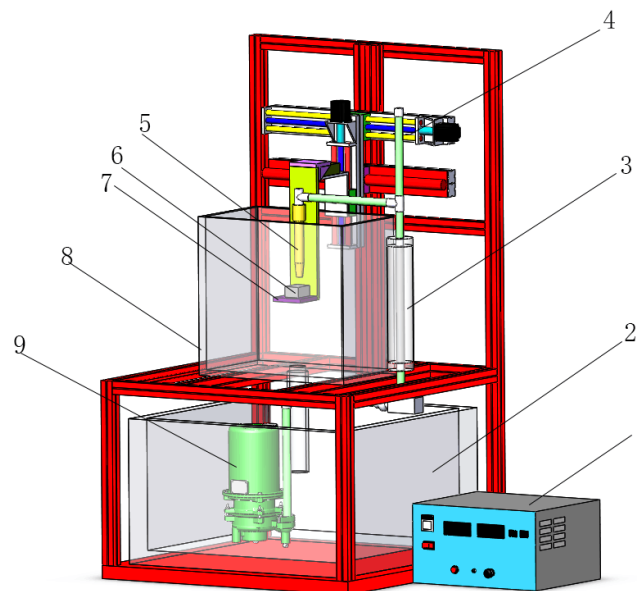
2. EXPERIMENTAL

2.1 Experimental system

A mild steel substrate with dimension of 30 mm×20 mm×5 mm was utilized as the cathode, whereas the anode was a pure nickel nozzle (chemical composition: 0.01% Fe, 99.98% Ni, 0.006% C, 0.001% Cu and 0.003% Si). Table 1 comprises the utilized plating solution and parameters to produce the Ni-SiC thin coatings. The solution was usually dispensed by mixing with all chemicals in a plating tank and adding deionized water to ensure 50 litres of bath. The experimental system for producing Ni-SiC thin coatings is demonstrated in Fig. 1. This system was designed by an industrial designer (*Ms. Kedi Jiang*), which was made up of power supply (SMD-60), bath recovery tank, fluid meter, electric regulation system, insulated operating platform, plating tank and circulating pump (CQB30-6A). During JPED, the bath recovery tank and plating tank were used to collect and store plating bath. The fluid meter was a LLJ-100 glass rotameter used for jet rates collection of plating bath. Distance between the nozzle and mild steel substrate (around 180 mm) was regulated by applying the electric regulation system. While insulated operating platform was used for the steel substrate fixation. Bath driving at a JV of 3 m³/h maintained by using a circulating pump.

Table 1. The plating bath composition and parameters for Ni–SiC thin coatings electrodeposition.

Compositions and conditions	Parameters
NiSO ₄ ·6H ₂ O	250 g/l
NiCl ₂ ·H ₂ O	29 g/l
H ₃ BO ₃	26 g/l
C ₃ H ₆ O ₃	4 g/l
SiC nanoparticles (average size ~20 nm)	10 g/l
CTAB surfactant	0.8 g/l
Plating temperature	50°C
pH	4.6
Current density	4 A/dm ²
Pulse frequency	500 Hz
Duty cycle	40%
Jet rate	1, 3, and 6 m/s
Electroplating time	60 min



1--Power supply, 2--Bath recovery tank, 3--Fluid meter, 4--Electric regulation system, 5--Nickel nozzle, 6--mild steel substrate, 7--Insulated operating platform, 8--Plating tank, 9--Circulating pump

Figure 1. Experimental installation for depositing Ni–SiC thin coatings.

2.2 Characterization

The 3D surface topographies and microstructures of the Ni–SiC thin coatings were separately watched by SPM (Nanoscope IIIa) and TEM (Tecnai-G2-20-S-Twin). The composition of the coating was tested by XRD instrument (Rigaku D/Max-2400) with Cu K α radiation ($\lambda=0.15418$ nm). By using

equation (1), the mean sizes of the Ni-SiC thin coatings were assessed:

$$D = \frac{180K\lambda}{\pi\sqrt{\beta^2 - FWHM \cos \theta}} \quad (1)$$

where, D is the mean size of the Ni perpendicular to the direction of the reflecting surface (hkl), K is a constant ($K=0.90$), β is the half-height width of the diffraction peak, θ represents the Bragg angle while full width at half maximum is represented by FWHM.

ANSYS software was used to simulate the jet velocity (JV) and kinetic energy (KE) of the bath. The Vickers hardnesses of the Ni-SiC thin coatings were determined at 15 s loading time using a HV-1500 durometer. In addition, the applied load on the coating material was 490, 980 and 7840 N, respectively. The wear and friction test was carried out on a MR-3G wear testing machine under the condition of no lubrication, in which a disc containing hardened steel ball was rotated at 100 rpm for 60 min. Each Ni-SiC coating was ultrasound-cleaned with deionized water before and after testing. The weight loss of each coating material was then calculated by an electronic balance (BLD250A). The worn morphology was studied through SEM. A CS350 electrochemical workstation was employed to carry out electrochemical impedance spectroscopy (EIS) tests in 3.5 wt.% NaCl etchant solutions.

3. RESULTS AND DISCUSSION

3.1 Kinetic energies of the plating solution

Fig. 2 displays the jet rate impact on the plating solution KE during the deposition of Ni-SiC thin coatings. Figs. 2a~2c simulate the jet rate of the plating bath, while Figs. 2a'~2c' simulate the KEs of the plating bath. It was observed that increase in the jet rate results in increased KE of the plating bath. At 1 m/s, the highest value of KE which is equivalent to $4.50 \text{ m}^2/\text{s}^2$ was generated in the center of the matrix. Furthermore, the highest value of KE was an increase to $15.2 \text{ m}^2/\text{s}^2$ at 3 m/s (Fig. 2b and b') while it was $39.1 \text{ m}^2/\text{s}^2$ at a jet rate of 6 m/s (Figs. 2c and c').

As is known to all [16], the KE can be calculated using Eq. (2):

$$K = \frac{3}{2}(VI)^2 \quad (2)$$

where, K shows the "KE" and V shows the "JV" of the plating solution while I shows the turbulence intensity of the plating solution.

According to Eq. (2), the KE was proportional to the square of the jet rate. i.e. with an increase in the jet rate of the plating bath increased, the KE of plating bath also increased directly. The results are consistent with the report explicated by Xia *et al.* [17].

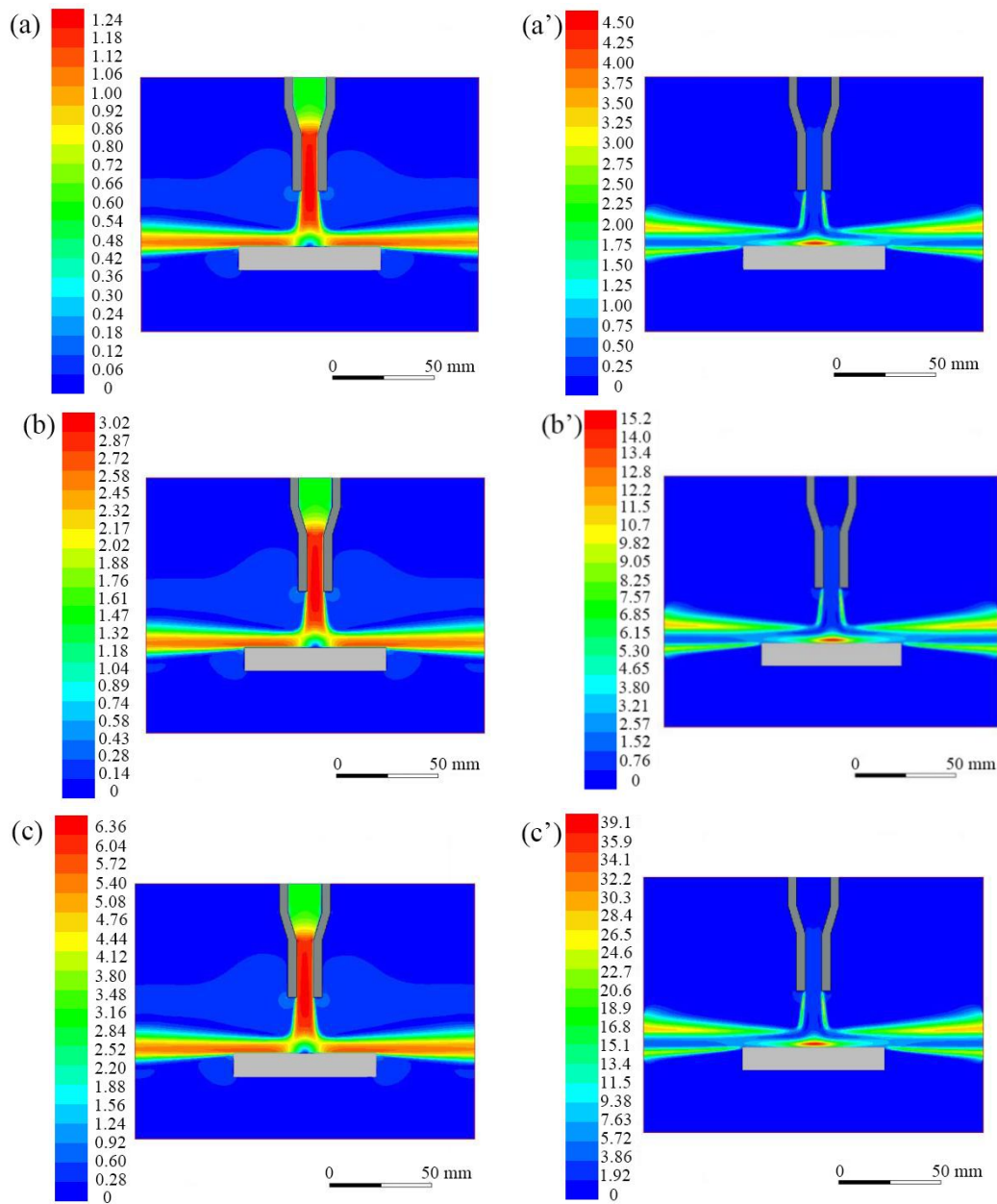


Figure 2. The jet rates and kinetic energies of the plating bath for depositing Ni–SiC thin coatings: (a) and (a') 1 m/s, (b) and (b') 3 m/s, (c) and (c') 6 m/s. (current density 4 A/dm², pulse frequency 500 Hz, and duty cycle 40%)

3.2 TEM and SPM images of Ni–SiC thin coatings

Fig. 3 shows the Ni–SiC thin coating microstructure formed at different jet rates. In Fig. 3a~c, the yellow part denotes Ni grains and the black part denotes SiC nanoparticles (NPs). The Ni–SiC coating deposited at 3 m/s showed smaller Ni particle size than that of the coatings deposited at 1 and 6 m/s. Additionally, when the jet rate was 3 m/s, the deposited coatings presented a compact and fine structure with a mean Ni size of 49.1 nm and SiC size of 18.4 nm.

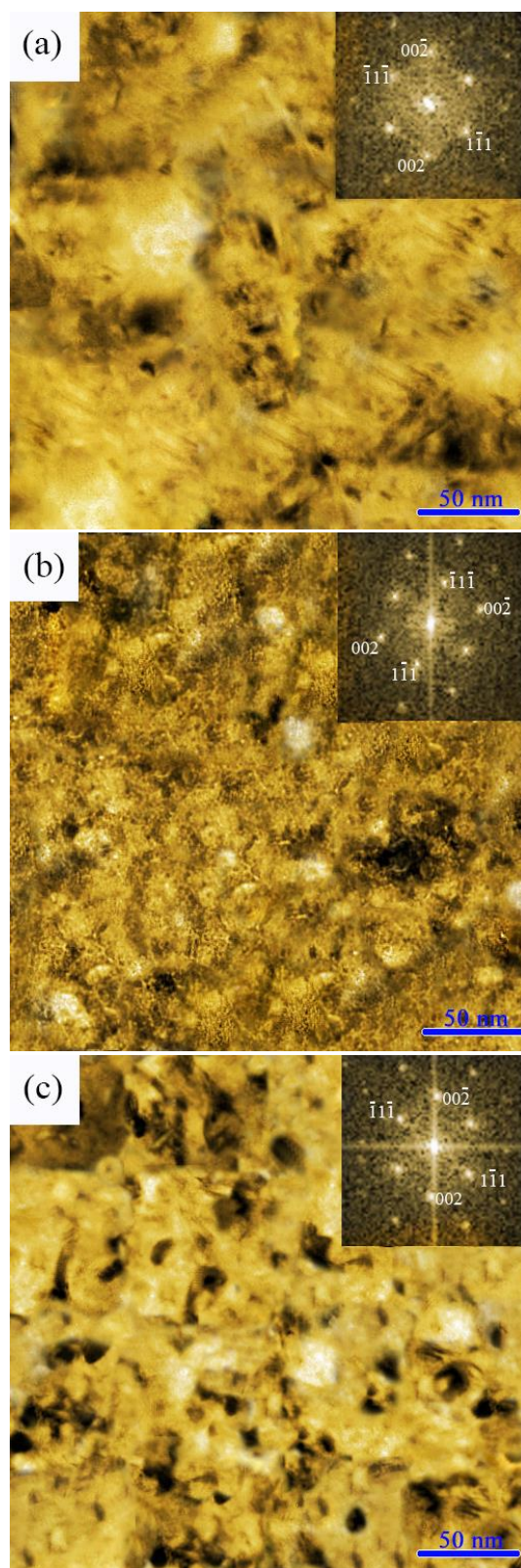


Figure 3. TEM images of Ni–SiC thin coatings produced at different jet rates: (a) 1 m/s, (b) 3 m/s, and (c) 6 m/s. (current density 4 A/dm², pulse frequency 500 Hz, and duty cycle 40%)

Fig. 4 shows the influence of jet rate on the SPM images of the Ni–SiC thin coatings which indicated a significant change in the surface morphologies of the Ni–SiC thin coatings. As shown in Figs.

4a and c, there were few SiC-NPs and obvious agglomeration phenomenon in thin coatings, and both thin coatings showed cauliflower-like crystal structures with larger size in the micro-areas.

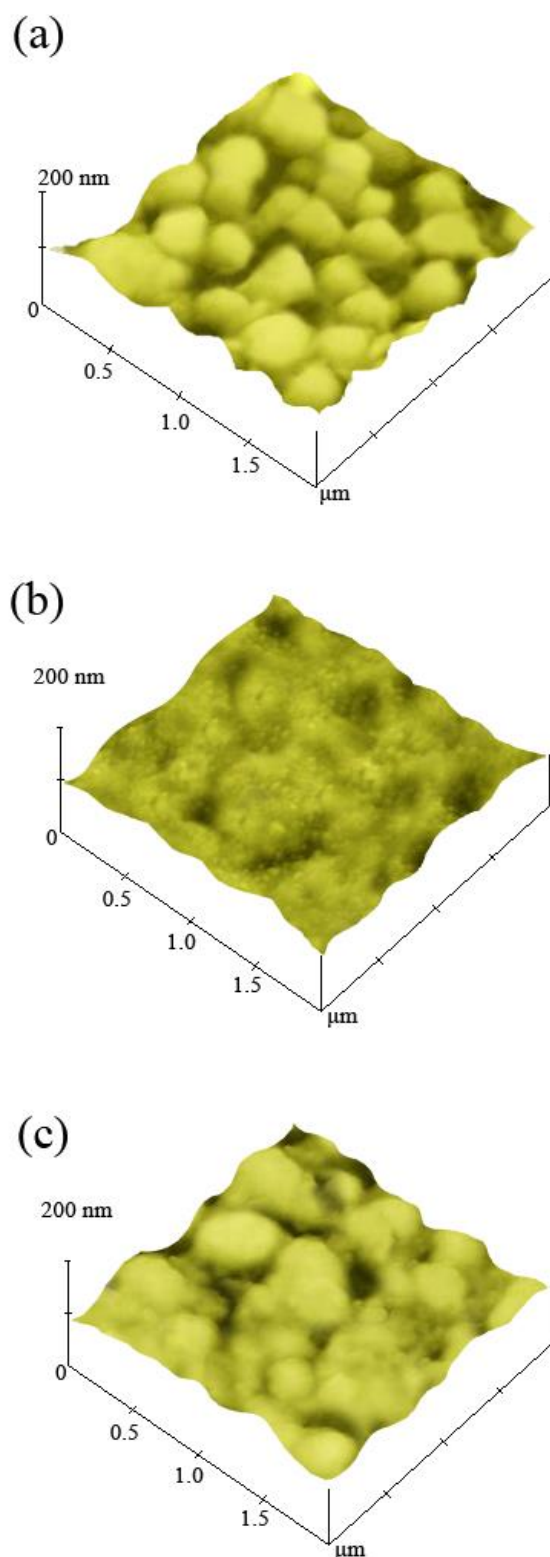


Figure 4. SPM images of Ni-SiC thin coatings produced at different jet rates: (a) 1 m/s, (b) 3 m/s, and (c) 6 m/s. (current density 4 A/dm², pulse frequency 500 Hz, and duty cycle 40%)

On the contrary, at 3 m/s jet rate, the resulting coatings had smooth and exiguous morphologies, and a large number of SiC NPs with ultra-fine structures were embedded in the Ni-SiC coating. The results are theoretically the same as the outcomes described by Sun *et al.* [18].

The reason behind this phenomena could be uniform dispersion of the SiC-NPs in both the plating solution as well as Ni-SiC coatings due to the suitable jet rate, which increased the coating content of SiC. These SiC-NPs are reported to increase the Ni grains nucleation number and hindered the nickel grains growth [19]. However, at a lower jet rate (e.g., 1 m/s), the KE of the electroplating bath did not inhibit the accumulation of SiC-NPs. Therefore, these micron-sized SiC-NPs were inserted into the coating obtained at 1 m/s, causing numerous nickel cores to further grow in size in Ni-SiC coatings. In addition, a gradual increase in jet velocity to 6 m/s, enhance the plating bath kinetic, leading to a significant increase in the jet liquid dispersion on SiC-NPs, thus flushing the SiC-NPs into the bath. This brought about the further growth of a large number of nickel grains, and increased the the degree of coarsening of Ni-SiC coatings.

3.3 XRD images of Ni-SiC thin coatings

Fig. 5 reveals the XRD image of SiC-NPs before JPED electroplating. The SiC particles could be exhibited from the corresponding diffraction peaks of the planes (1 1 1), (2 0 0) and (2 2 0) at 34.1°, 41.4°, and 59.6°, respectively.

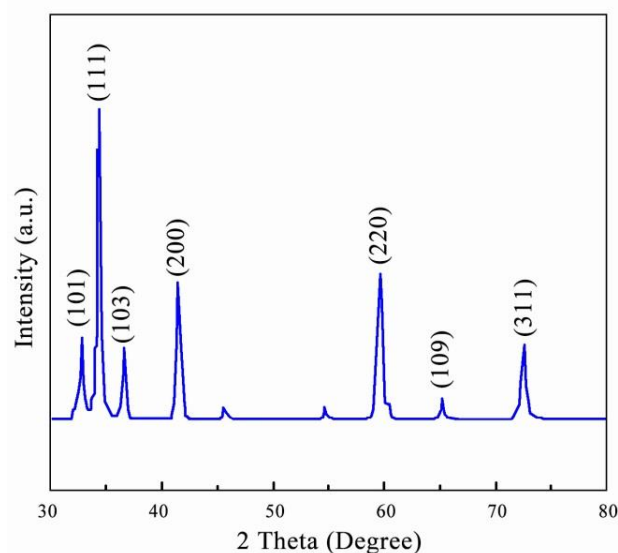


Figure 5. XRD image of SiC nanoparticles.

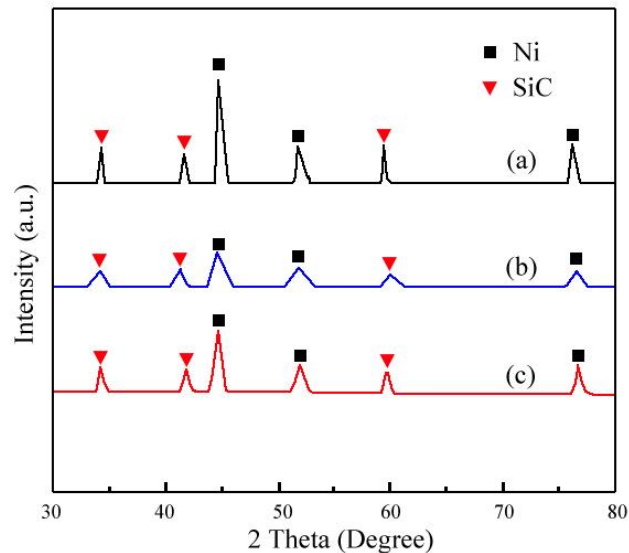


Figure 6. XRD images of Ni–SiC thin coatings produced at different jet rates: (a) 1 m/s, (b) 3 m/s, and (c) 6 m/s. (current density 4 A/dm², pulse frequency 500 Hz, and duty cycle 40%)

Besides, the XRD spectrogram also showed four low-dimensional peaks (2θ is equal to 32.7°, 36.5°, 65.4°, and 72.6°), which were determined as the (1 0 1), (1 0 3), (1 0 9) and (3 1 1) SiC particles planes, respectively. Fig. 6 shows the XRD patterns of the Ni-SiC thin coatings obtained by JPED technology at different JVs. The JV was favorable for SiC-NPs to be embedded in the Ni-SiC thin coatings. In addition, with increasing jet rate from 1 m/s to 6 m/s, the Ni sizes in the thin coatings initially decreased and then increased slightly. At 3 m/s, the observed mean size of Ni and SiC in the JPED-deposited Ni-SiC coating was equivalent to 50.1 nm and 19.6 nm, respectively. While at 6 m/s, the mean Ni and SiC size was found to be 73.6 nm and 25.3 nm, respectively. The results were consistent with TEM and SPM results. This result is consistent with that reported by Xia *et al.*[20].

3.4 Microhardness of Ni–SiC thin coatings

Fig. 7 describes the Ni–SiC thin coatings microhardness in different applied loads. Table 2 shows the influence of jet rate on the value of microhardness of Ni–SiC thin coatings. Comparing the three kinds of Ni-SiC coatings, it was concluded that the highest microhardness was observed (884.5 HV) for Ni–SiC coating prepared under the condition of 3 m/s jet rate, while the coating prepared under the condition of 1 m/s showed the lowest microhardness which is about 729.5 HV. The content and distribution of the SiC-NPs embedded in the coatings had an important influence on the microhardness of Ni–SiC coatings. The moderate jet rate increased the SiC content of the coating, resulting in a compact and fine structure that enabled the coating to achieve the highest microhardness. Besides, the hardness of SiC-NPs was hard and uniformly dispersed, which could make the coating having uniform microhardness, thus enhancing the overall mechanical characteristics of Ni-SiC thin coatings. The phenomenon is consistent with the investigation explained by Xia *et al.* [21].

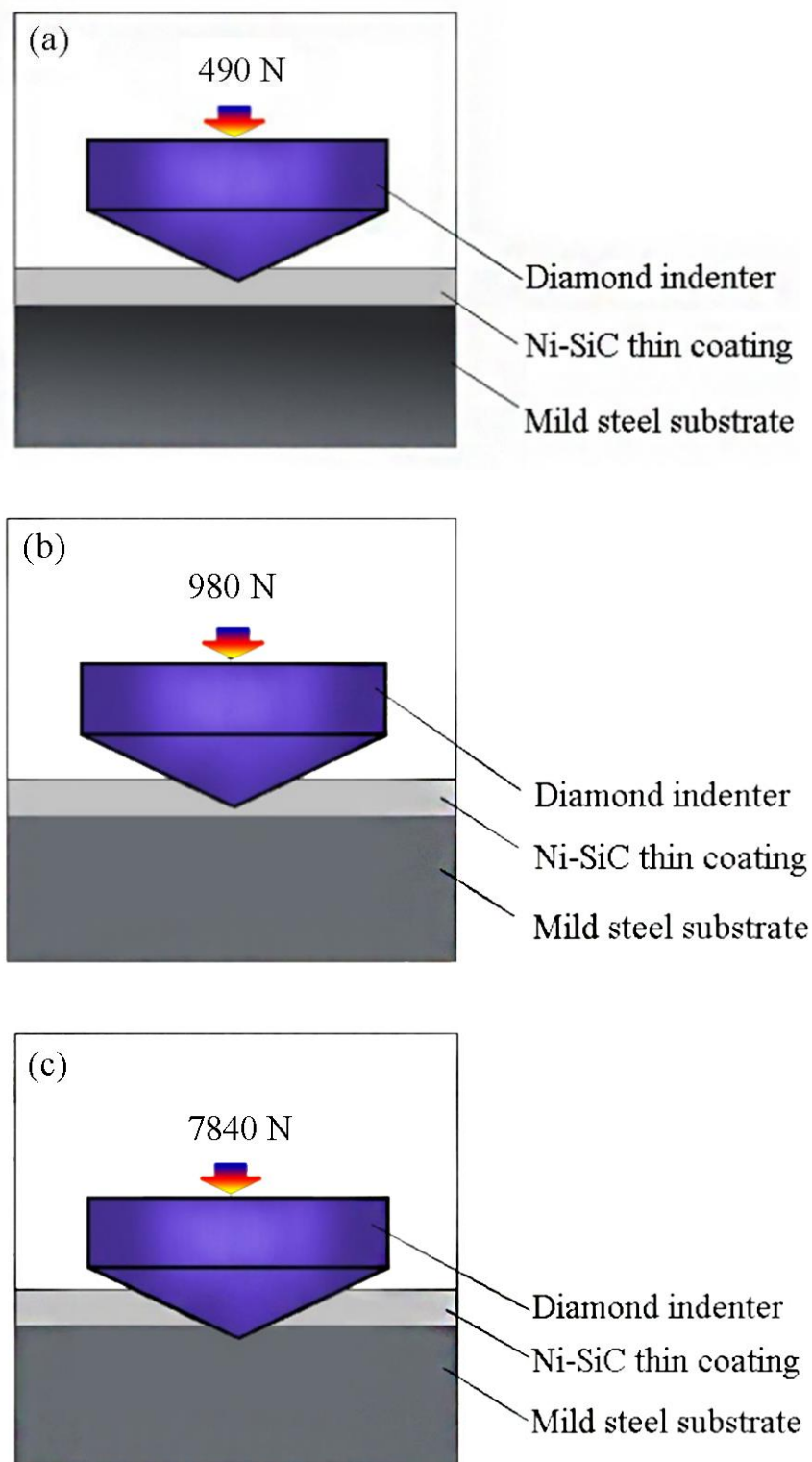


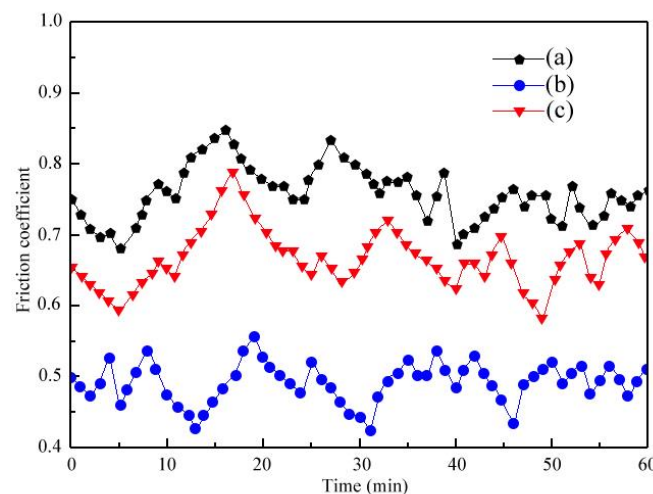
Figure 7. Schematic diagram for measuring the microhardness of Ni–SiC thin coatings under different applied loads: (a) 490 N, (b) 980 N, and (c) 7840 N.

Table 2. Effect of jet rate on the microhardnesses of Ni–SiC thin coatings (current density 4 A/dm², pulse frequency 500 Hz, and duty cycle 40%).

Jet rate (m/s)	Microhardness (HV)			
	490 N	980 N	Average	7840 N
1	728	731	729.5	330
3	875	894	884.5	329
6	812	828	820.0	326

3.5 Wear properties of Ni–SiC thin coatings

Fig. 8 depicts the relationship between the coefficient of friction (COF) of the Ni–SiC coatings and jet rate. The results revealed that the COF of the Ni–SiC coatings prepared under different jet rates were various in the friction and wear experiments. Among all the Ni–SiC coatings, the minimum COF was observed for Ni–SiC coating prepared at 3 m/s with a mean COF of about 0.49. On the contrary, the Ni–SiC coating at 1 m/s showed the largest COF (~0.75) compared with all other Ni–SiC thin coatings. Fig. 9 shows the variation in weight of Ni–SiC thin coatings before and after wear testing. Ni–SiC coating prepared under 3 m/s showed low weight loss (~0.36 g), while higher weigh losses for similar jet plating parameters was observed for Ni–SiC thin coatings obtained at 1 and 6 m/s. This result is consistent with the work depicted by Zhang *et al.* [22].

**Figure 8.** Effect of jet rate on friction coefficients of Ni–SiC composites: (a) 1 m/s, (b) 3 m/s, and (c) 6 m/s. (current density 4 A/dm², pulse frequency 500 Hz, and duty cycle 40%)

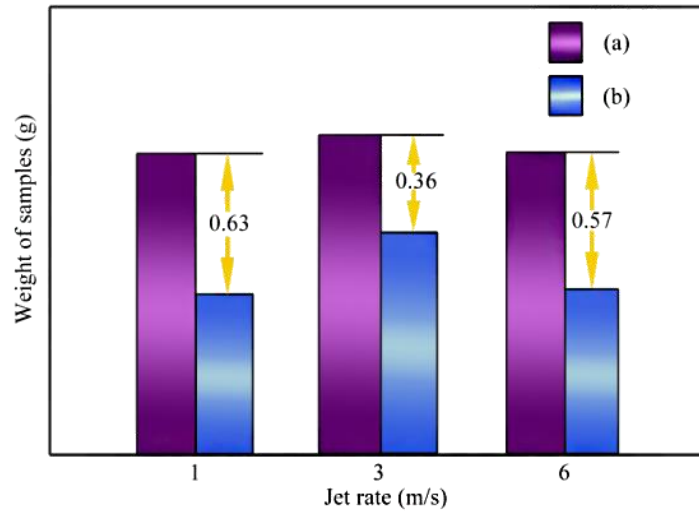
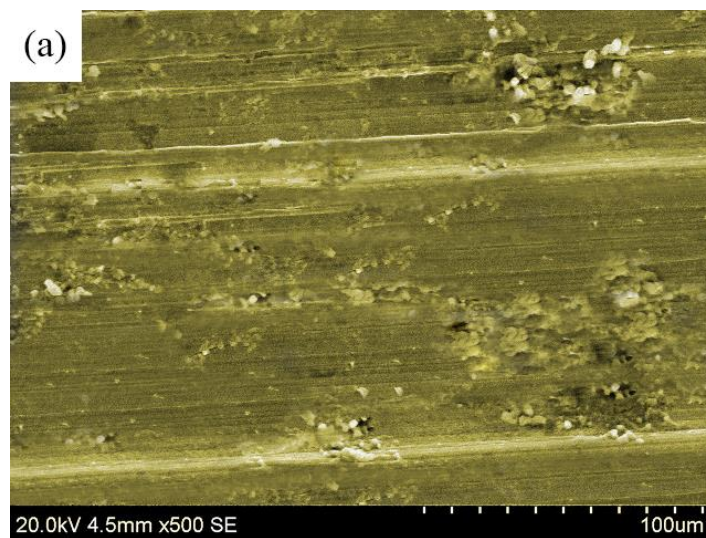


Figure 9. The weight changes of Ni-SiC thin coatings under different jet rates: (a) before wear test, (b) after wear test. (current density 4 A/dm², pulse frequency 500 Hz, and duty cycle 40%)

Fig. 10 presents the SEM results of the Ni-SiC thin coating wear surfaces prepared under varying jet velocities. There are obvious friction scratches in the Ni-SiC coatings produced at 1 and 6 m/s, with some deep grooves and larger pits on the coating surfaces. On the contrary, the coating obtained under the condition of 3 m/s showed slight scratches with some small-sized pits in the coating.



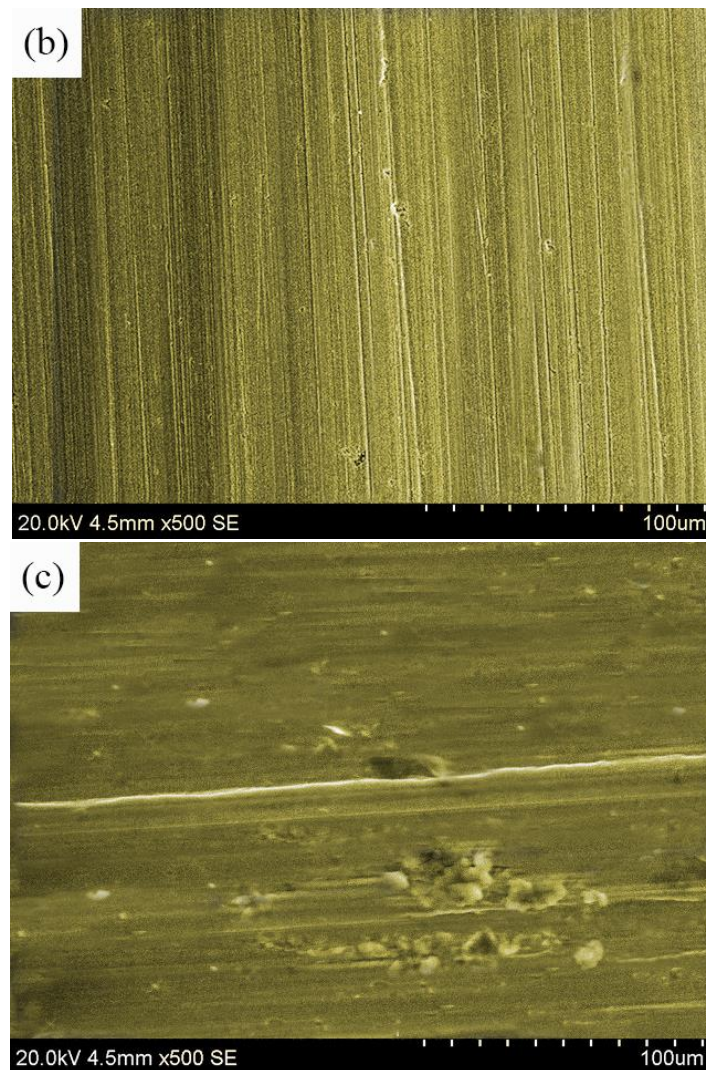


Figure 10. SEM micrographs of the worn surface of Ni–SiC thin coatings obtained at different jet rates: (a) 1 m/s, (b) 3 m/s, and (c) 6 m/s. (current density 4 A/dm², pulse frequency 500 Hz, and duty cycle 40%)

According to above-mentioned results, the mechanism of wearing Ni–SiC thin coatings was elaborated as: (1) Microstructure possess significant on the wear loss and COF of Ni-SiC coatings. When a suitable number of SiC-NPs with high microhardness value were doped into the Ni-SiC coatings to disperse in the matrix, the coatings became compact and fine, which resulted in a lower COF and reduced wear losses in wear tests. (2) The content and distribution of SiC-NPs are significantly affected by the jet rate. With moderate jet rate, the deposition of SiC-NPs was promoted, thus increasing the content of SiC in coatings. The SiC-NPs in the thin coatings could significantly inhibit any deep cutting of the coating surfaces. Therefore, at 3 m/s, the resulting coating had only slight scratches in certain numbers rather than large surface pits and deep grooves.

3.6 EIS measurements of Ni–SiC thin coatings

The measured Nyquist diagrams at varying jet rates on the deposited Ni–SiC thin coatings are displayed in Fig. 11. The lowest impedance was found for the Ni–SiC coating produced at 1 m/s, which testifies its worst anti-corrosion performance. On the contrary, the thin coating deposited at 3 m/s processed the highest impedance, indicating the best corrosion resistance among all coatings. The results are consistent with the investigation explicated by Ma *et al.* [23].

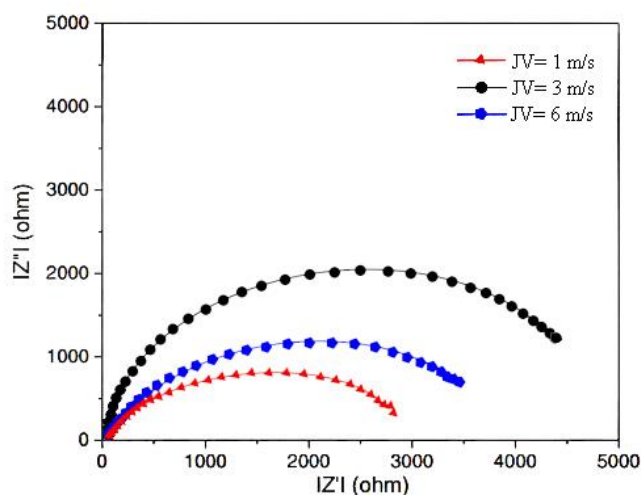


Figure 11. Nyquist curves of Ni–SiC thin coatings obtained at different jet rates: (a) 1 m/s, (b) 3 m/s, and (c) 6 m/s. (current density 4 A/dm², pulse frequency 500 Hz, and duty cycle 40%)

4. CONCLUSIONS

(1) The Ni–SiC thin coatings occurred at a jet velocity of 3 m/s showed a compact and fine structure, while SiC and Ni average size was observed as 18.4 nm and 49.1 nm respectively. A large number of SiC-NPs with ultra-fine structure were embedded in the coating.

(2) At 3 m/s JV, the maximum KE generated (15.2 m²/s²) in the center of the substrates. Besides, the KE of the plating bath would increase directly with the increase of the jet rate.

(3) XRD results revealed the diffraction peaks of the SiC particles at 34.1°, 41.4°, and 59.6°, corresponding to the (1 1 1), (2 0 0) and (2 2 0), respectively. The SiC and Ni average size in the Ni–SiC thin coatings prepared at a jet velocity of 3 m/s were separately 19.5 nm and 50.2 nm.

(4) The comparison of the three Ni–SiC thin coatings showed that at 3 m/s Ni–SiC coating showed the highest microhardness i.e. 884.5 HV, while the Ni–SiC coating at a jet rate of 1 m/s had the lowest average microhardness of 729.5 HV.

(5) The prepared Ni–SiC thin coatings at 3 m/s showed the lowest COF among all the Ni–SiC thin coatings, whereas the average COF was about 0.49. The coating obtained at a speed of 3 m/s had some fine scratches on the wear morphology, and only a certain number of small size pits appeared on

the coating surface. In addition, the Ni-SiC thin coating deposited at 3 m/s processed the highest impedance, indicating the best corrosion resistance among all coatings.

ACKNOWLEDGEMENT

This work has been supported by the National Natural Science Foundation of China (Granted no. 51974089), the Basic Scientific Research Operating Expenses of Undergraduate Universities in Heilongjiang Province - Project of Northeast Petroleum University's Leading Innovation Fund (Granted no. 2018YDL-08), and the Department of Education Innovation Strong School Project (Granted no. 2018KTSCX141).

DATA AVAILABILITY

The data that support the findings of this study are available from the corresponding author upon reasonable request.

References

1. F. Xia, Q. Li, C. Ma, W. Liu, and Z. Ma, *Ceram. Int.*, 46 (6) (2020) 7961.
2. F. Xia, M. Wu, F. Wang, Z. Jia, and A. Wang, *Curr. Appl. Phys.*, 9 (1) (2009) 44.
3. C. Ma, D. Zhao, H. Xia, F. Xia, Z. Ma, and T. Williams, *Int. J. Electrochem. Sci.*, 15 (2020) 4015.
4. S.C. Jambagi, and P.P. Bandyopadhyay, *J. Mater. Eng. Perform.*, 28 (12) (2019) 7347.
5. N.P. Wasekar, S.M. Latha, M. Ramakrishna, D.S. Rao, and G. Sundararajan, *Mater. Des.*, 112 (2016) 140.
6. S.A. Lajevardi, T. Shahrabi, and J.A. Szpunar, *Appl. Surf. Sci.*, 279 (2013) 180.
7. Y.X. Li, P.F. Zhang, P.K. Bai, L.Y. Wu, B. Liu, and Z.Y. Zhao, *Surf. Coat. Technol.*, 334 (25) (2018) 142.
8. F.F. Xia, J.Y. Tian, C.Y. Ma, M. Potts, and X. Guo, *J. Appl. Phys.*, 116 (23) (2014) 234301.
9. R.S. Mane, and C.D. Lokhande, *Mater. Chem. Phys.*, 65 (1) (2010) 1.
10. X.H. Zheng, M. Wang, H. Song, D. Wu, X.T. Liu, and J. Tan, *Surf. Coat. Technol.*, 325 (2017) 181.
11. Y.H. Kim, K.S. Lee, T.S. Lee, B. Cheong, T.Y. Seong, and W.M. Kim, *Appl. Surf. Sci.*, 255 (16) (2009) 7251.
12. F.F. Xia, W.C. Jia, C.Y. Ma, R. Yang, Y. Wang, and M. Potts, *Appl. Surf. Sci.*, 434 (2018) 228.
13. C. Ma, W. Yu, M. Jiang, and F. Xia, *Ceram. Int.*, 44 (5) (2018) 5163.
14. Z.J. Tian, D.S. Wang, G.F. Wang, L.D. Shen, Z.D. Liu, and Y.H. Huang, *T. Nonferr. Metal. Soc.*, 20 (6) (2010) 1037.
15. R. Cui, R. Wang, C. Peng, and C. Dong, *Al. Process.* 3 (2019) 14. (In Chinese)
16. S.Y. Wang, X.X. Jiang, R.C. Wang, X. Wang, S.W. Yang, J. Zhao, and Y. Liu, *Adv. Powder. Technol.*, 28 (6) (2017) 1611.
17. F. Xia, C. Li, C. Ma, Qiang Li, and H. Xing, *Appl. Surf. Sci.*, 538 (2021) 148139.
18. C. Sun, X. Liu, C. Zhou, C. Wang, and H. Cao, *Ceram. Int.*, 45(1) (2019) 1348.
19. C.Y. Ma, D.Q. Zhao, and Z.P. Ma, *Ceram. Int.*, 46 (8) (2020) 12128.
20. F. Xia, Q. Li, C. Ma, and X. Guo, *Ceram. Int.*, 46 (2) (2020) 2500.
21. F. Xia, J. Tian, W. Wang, and Y. He, *Ceram. Int.*, 42 (2016) 13268.
22. J. Zhang, J. Lei, Z. Gu, F. Tantai, and Y. Fang, *Surf. Coat. Tech.*, 393 (2020) 125807.
23. C. Ma, M. Jiang, and F. Xia, *Surf. Rev. Lett.*, 24 (2016) 17500631.